search Council, Washington, D.C., 1979, pp. 59-72.
4. R.A. Weiss. Pavement Evaluation and Overlay Design: A Method that Combines Layered-Elastic Theory and Vibratory Nondestructive Testing. In Transportation Research Record 700, TRB, National Research Council, Washington, D.C., 1979, pp. 20-34.
5. H.J. Treybig. Mechanistic Method of Pavement Overlay Design. In Transportation Research Record 700, TRB, National Research Council, Washington, D.C., 1979, pp. 72-77.
6. AASHO Committee on Design. Interim Guide for the Design of Flexible Pavement Structures. AASHO, Washington, D.C., Oct. 12, 1961.
7. W.J. Kenis. Predictive Design Procedures, VESYS User Manual--An Interim Design Method for Flexible Pavements Using VESYS Structural Subsystem. Final Report. FHWA, U.S. Department of Transportation, Jan. 1978, 128 pp.
8. The AASHO Road Test: Report 5--Pavement Research. Special Report 61E, HRB, National Research Council, Washington, D.C., 1962, 352 pp.

Publication of this paper sponsored by Committee on Pavement Rehabilitation.

Nondestructive Testing of Pavements Using Surface Waves

SOHEIL NAZARIAN and KENNETH H. STOKOE II

ABSTRACT

A nondestructive method of determining the moduli and thicknesses of pavement systems--the spectral-analysis-of-surface-waves (SASW) method--was introduced in 1982. With this method surface waves containing a wide range in frequencies are generated in the pavement system by impacting the surface. Propagation of the waves through the system is monitored with two receivers located on the pavement surface. By analysis of the phase information for each frequency determined between receivers, Rayleigh wave velocities and wavelengths over the frequency range of interest are determined. Velocity versus wavelength information represents a dispersion curve that on inversion gives Young's modulus profiles along with the thicknesses of the layers. Advancements in the theoretical aspects of the inversion method are presented in this paper. A new, rigorous inversion technique has been developed that is theoretically based and eliminates many of the earlier simplifying assumptions. The versatility and accuracy of the new inversion technique is illustrated by two series of tests that were performed on two rigid pavement sections of an airport runway with different cross-sectional profiles. In addition to being nondestructive, fast, and economical, the SASW method is shown to be capable of detecting thin layers in pavement systems with an accuracy of less than 0.5 in. and finding moduli within about 20 percent, based on comparisons with soil borings and crosshole seismic tests at the same sites. In this regard, no other nondestructive technique has the power and versatility of this method.

Many major highways and airport runways are approaching the end of their serviceable lives. A fast, economical, and precise method for evaluating the properties of these pavements is necessary if meaningful maintenance inspections are to be performed regularly or if overlays are to be designed effectively. The most common nondestructive tests (NDTs) being performed for these purposes are the Dynaflect and the falling weight deflectometer. Although these tests are carried out quite rapidly in situ, in-house data processing can be tedious, and the final solutions are not unique. Another potential deficiency with these methods is that, although a dynamic load is applied to the surface in the field, static elastic theory is employed to reduce the data. Under certain conditions, stress and strain distributions in these dynamic tests can be different from those assumed in the static analyses.

The latest developments in the spectral-analysis-of-surface-waves (SASW) method are discussed herein. The SASW method, which has been under development for some time (1-4), is a nondestructive testing technique that is based on the theory of elastic waves in a layered system. In addition to elastic moduli, layer thicknesses can be determined precisely from the modulus profile. A brief overview of the SASW testing technique is presented herein, followed by recent developments in data analysis that are needed for achieving high-quality Young's modulus profiles and precise layer thicknesses. The results of a case study on two rigid pavement sections using the rigorous data reduction technique are presented to illustrate the value of the SASW method. In conjunction with SASW tests, crosshole seismic tests were performed at each site. Crosshole tests are known as a precise way of determining the stiffnesses of different layers at a site. Young's modulus profiles obtained from these two tests are in excellent agreement, as are the layer thicknesses obtained from the SASW tests and borings.

BACKGROUND

SASW Method

The SASW method is a new method of seismic testing that is being developed for determining shear wave velocity and shear modulus profiles at soil sites and Young's modulus profiles at pavement sites (3,4). Evaluation of Young's modulus profiles at pavement sites can be used in overlay design or material characterization (5) or the profiles can be used indirectly as a tool to control compaction during construction (6). All testing is performed at the ground surface, and hence the procedure is nondestructive. The key point in SASW testing is generation and measurement of surface waves (Rayleigh waves).

The source is simply a transient vertical impact on the pavement surface. The impact generates a group of Rayleigh waves (R-waves) of various frequencies. Two vertical receivers, located on the surface, are used to monitor the propagation of Rayleigh wave energy past them. The output from the receivers is simultaneously captured and recorded on a Fourier spectral analyzer. With the Fourier analyzer, the complicated transient waveforms are divided into a group of simple harmonic waveforms that are analyzed to determine wave velocity and moduli.

The general configuration of the source, receivers, and recording device is shown in Figure 1a. The common receivers midpoint (CRMP) geometry (4) is used for testing. With this geometry, the two receivers are moved away from an imaginary centerline midway between the receivers at an equal pace, and the source is moved such that the distance between the source and the near receiver is equal to the distance between the two receivers. In addition, the location of the source is reversed for each receiver spacing so that forward and reverse profiles are run. By averaging the forward and reverse profiles, the effect of any internal phase between receivers is eliminated. This testing sequence is shown in Figure 1b. As the method is still in research stages, testing time at each site is approximately 30 min. However, after the testing procedure is automated, the testing period will be only minutes, and thus comparable with other NDT methods.

By analysis of phase information for each frequency determined between the two receivers, Rayleigh wave velocity, shear wave velocity, and eventually Young's modulus are determined. Rayleigh wave velocity (V_R) is constant in a homogeneous halfspace and is independent of frequency. Each frequency (f) has a corresponding wavelength (L_R) according to

$$V_R = f \cdot L_R \quad (1)$$

Rayleigh wave and shear wave velocities are related by Poisson's ratio. The ratio of R-wave to S-wave velocity varies slightly with Poisson's ratio but can be assumed equal to 0.90 with an error of less than 5 percent.

If the stiffness of a site varies with depth, then the velocity of the Rayleigh wave will vary with frequency. The variation of R-wave velocity

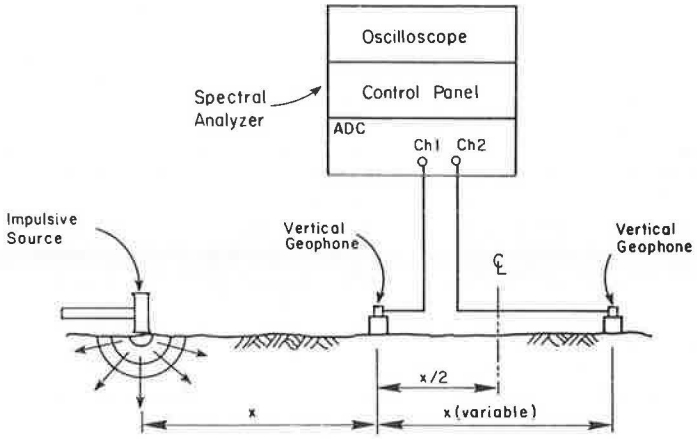

(a) General Configuration of SASW Tests

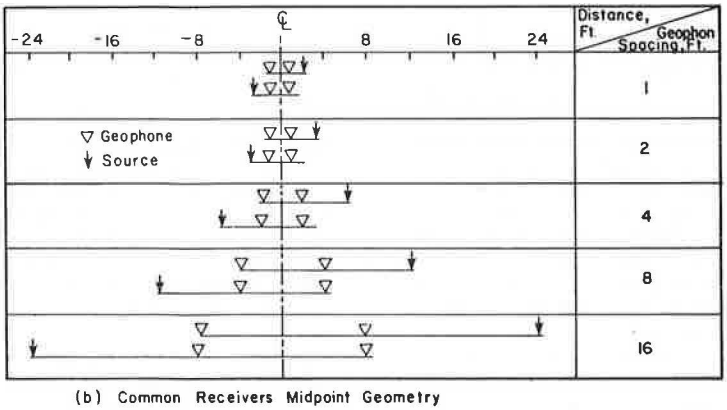

(b) Common Receivers Midpoint Geometry

FIGURE 1 Schematic of experimental arrangement for SASW tests.

with frequency (wavelength) is known as dispersion, and a plot of velocity versus wavelength is called a dispersion curve. The dispersion curve is constructed based on data collected in the field.

Inversion of the R-wave dispersion curve is the procedure of determining the actual propagation velocities at different depths from the dispersion curve. Inversion consists of determination of the depth and shear wave velocity of each layer from the R-wave velocity versus wavelength data. Inversion is the most important stage in determining a meaningful profile by the SASW method, and inversion is discussed in detail herein.

Crosshole Seismic Test

A second seismic test--the crosshole test--was used in the field to develop independently modulus profiles to compare with the SASW results. The basic concept of the crosshole test involves measurement of body waves (compression and shear) propagating along horizontal travel paths at different depths in the medium. Propagation velocities at these depths are calculated once travel times and distances have been measured. By means of elastic theory, moduli of each layer are then evaluated. The thicknesses of the layers are determined from the borings used in the crosshole test.

A schematic of the crosshole testing procedure used at the pavement sites is shown in Figure 2. The borehole array at each site consisted of three boreholes arranged in a linear array with approximately 3.5-ft spacing between adjacent boreholes. Each borehole was advanced to the appropriate measurement depth by using solid-stem augers. At each testing depth the drilling operation was stopped and the source was placed in the bottom of one hole. The receivers were located at the same depth in the other holes. A vertical impulse, which simultaneously activated the recording device, was then applied to the source. The impulse was detected by receivers in the other holes as the body waves passed. The source consisted of a sampling tube attached to a 1-in.-diameter rod. A vertical velocity transducer secured to the rod just above the sampling tube served as the trigger for the recording device. The receivers consisted of three-dimensional velocity transducers.

A typical record detected with the vertical geophone at a distance of 3.5 ft from the source is shown in Figure 3a. The upper portion of the figure is the impulse monitored by the source geophone. A time delay was used at the beginning of the record so that the triggering point could be easily distinguished (marked as I on the record). The lower part of the figure shows the record of body waves monitored by the vertical geophone. The direct P- and S-wave arrivals are marked by P and S, respectively. Shear and compressional travel times are simply the time differences between point I and points S or P, respectively. Although P-wave velocity can be identified on this record, it is preferred that this velocity be determined from a record obtained by using a transducer that is oriented in the direction of propagation (i.e., a radial, horizontal geophone). A typical travel time record monitored with a radial, horizontal geophone is shown in Figure 3b. The triggering time and direct arrival of the P-wave are marked as I and P, respectively. The amplitude on the travel time record of the P-wave is larger and easier to identify in Figure 3b than in Figure 3a because of the proper orientation of the receiver.

Propagation velocity is determined simply by dividing the distance between the source and receiver by the travel time over this distance. Moduli and Poisson's ratio are then determined according to elastic theory as

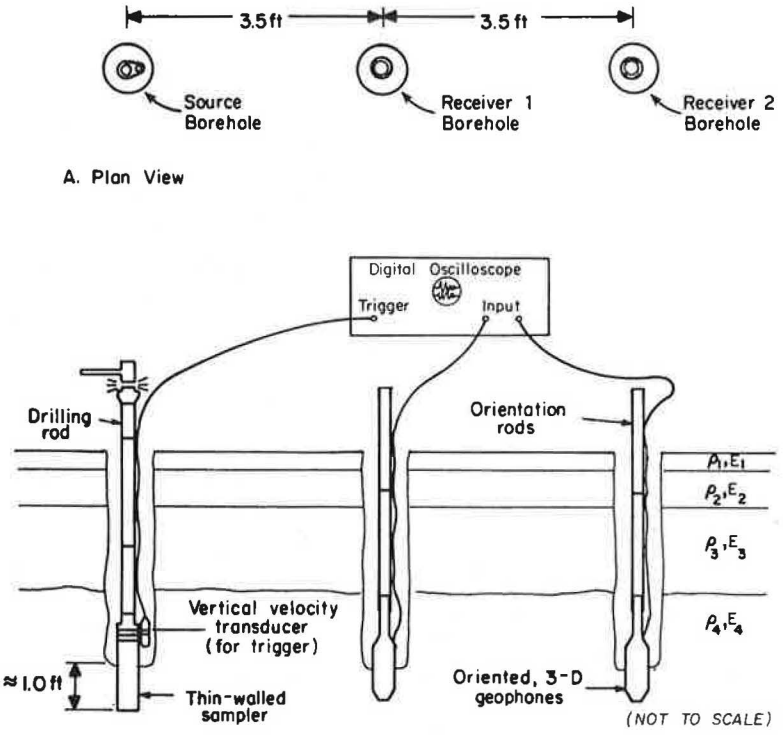

FIGURE 2 Crosshole testing technique used at runway sites.

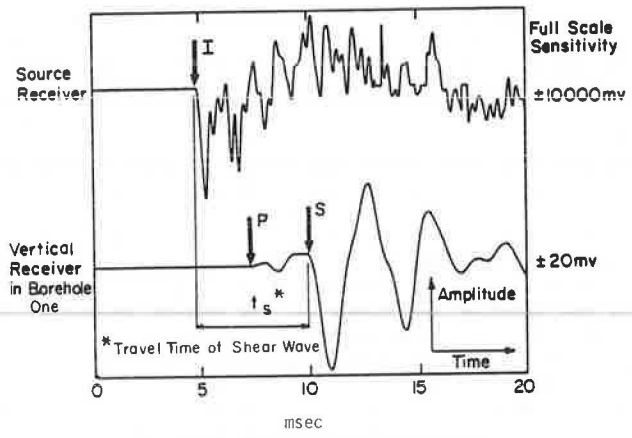

a) Travel Time Record of Shear Wave

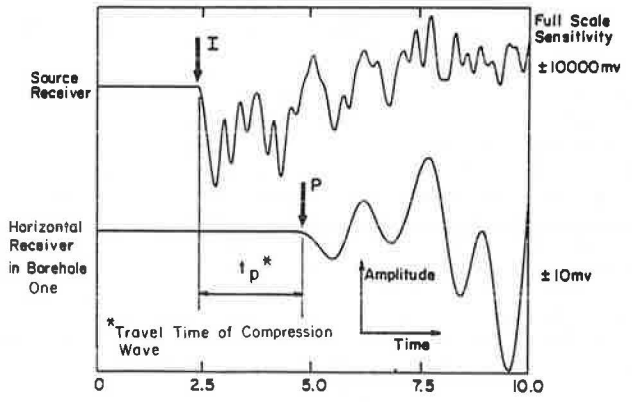

b) Travel Time Record of Compression Wave

FIGURE 3 Typical travel time records generated with vertical impulses in crosshole seismic test.

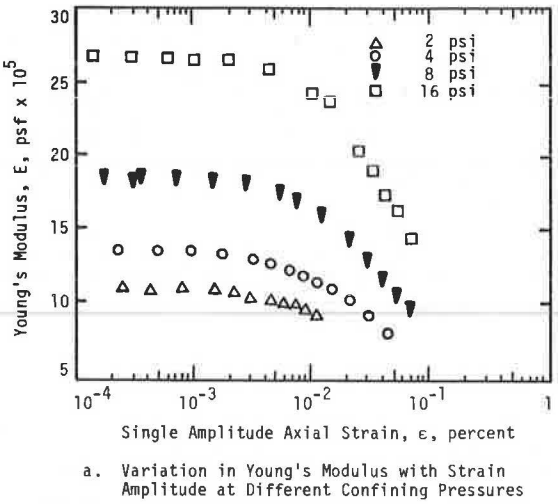

a. Variation in Young's Modulus with Strain Amplitude at Different Confining Pressures

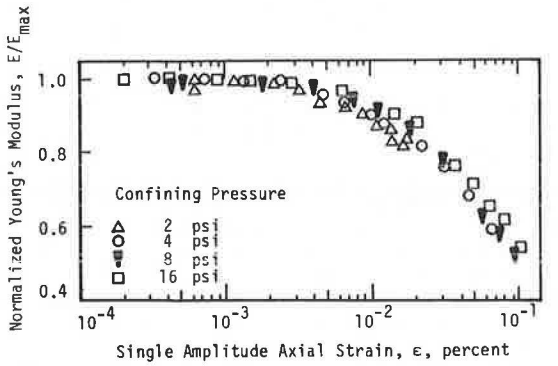

b. Variation in Normalized Young's Modulus with Strain Amplitude

FIGURE 4 Effect of axial strain amplitude on Young's modulus of an unsaturated clay subgrade.

$$G = (\gamma/g)V_S^2 \quad (2)$$

$$E = (2\gamma/g)V_S^2 (1 + \nu) = (\gamma/g)V_P^2 \times \{[(1 + \nu)(1 - 2\nu)]/(1 - \nu)\} \quad (3)$$

$$M = (\gamma/g)V_P^2 \quad (4)$$

$$\nu = [0.5(V_P/V_S)^2 - 1]/[(V_P/V_S)^2 - 1] \quad (5)$$

where

V_P = compression wave velocity,
V_S = shear wave velocity,
G = shear modulus,
E = Young's modulus or modulus of elasticity,
M = constrained modulus,
γ = total unit weight of the material,
g = gravitational acceleration, and
ν = Poisson's ratio.

Values of these parameters determined from seismic measurements represent the material behavior at small shearing strains, that is, strains less than 0.001 percent (7). In this strain range material behavior, particularly subgrade material, is typically independent of strain amplitude.

A typical example of the variation in E with normal strain (ε) for subgrade is shown in Figure 4. An undisturbed sample of unsaturated clay from San Antonio, Texas, was tested by using the resonant column method (8). The variation in E with log ε at several confining pressures is shown in Figure 4a. It is evident that, below strains of about 0.001 percent, E is constant and independent of strain at each pressure.

The effect of strain on modulus is easily seen by plotting the variation of normalized modulus (E/E_{max}) with log ε, as shown in Figure 4b. In Figure 4b, E_{max} is taken as the maximum value of Young's modulus at each confining pressure and is often termed the low-amplitude modulus or elastic modulus. Note that Young's modulus is constant below a strain of about 0.001 percent and is equal to E_{max}. As such, any seismic measurement in which modulus is measured at strains below about 0.001 percent results in measurement of a strain-independent modulus (E_{max}). This is a beneficial characteristic of seismic measurements in that different techniques, if properly performed, result in essentially the same value of modulus, E_{max}. In addition, if a normalized modulus versus strain curve such as that shown in Figure 4b is available for the material, then the reduced modulus in the nonlinear range can be determined once E_{max} has been measured seismically.

EXPERIMENTS ON RIGID AIRPORT PAVEMENTS

The SASW method was used at two sites in the apron area of Tyndall Air Force Base (AFB) near Panama City, Florida, in June 1983. The method was used to

determine the variation of in situ shear wave velocity and Young's modulus with depth for two pavement systems. In conjunction with SASW testing, crosshole tests were also performed as previously described. The crosshole tests were conducted so that Young's modulus profiles could be compared with those determined by SASW tests at each site.

Location

Two sites were tested in the apron area at Tyndall AFB. An overview of the sites and the test locations is shown in Figure 5. The apron consists of two different pavement sections constructed at different times. Slabs A and B in Figure 5 correspond to old and new pavements, respectively.

The old pavement, which was constructed during the World War II era, consists of approximately 6 in. of unreinforced concrete underlain by sand. The dimensions of individual slabs in this area are 10 ft by 15.5 ft. The new pavement, which was constructed recently, consists of approximately 10 in. of unreinforced concrete underlain by approximately 4 in. of cement-treated base and then natural sand. This area is divided by sawed joints into slabs about 14.5 ft wide and 25.5 ft long. No significant cracking was evident within the slabs tested at either location.

Procedure

The testing procedure (shown in Figure 1) was carried out at each site. Vertical geophones with a natural frequency of 4.5 Hz were used. Also, a series of back-up data was collected at each site by using geophones with a natural frequency of 2 Hz. In the case of the old pavement, geophone spacings of 1, 2, 4, 8, 14, and 24 ft were used. The closer spacings were used to sample near-surface material, and the larger spacings were used to sample deeper materials. As shallower depths correspond to higher frequencies, a frequency range of 0 to 12,800 Hz was selected for the geophone spacing of 1 ft. The upper limit of this frequency range was then decreased as the spacing increased to a final limit of 400 Hz at the 24-ft spacing.

Geophone spacings used on the new pavement were 1, 2, 4, 8, 16, and 32 ft, and the frequency limits were similar to those used at the old pavement. Different sources were also used with different geophone spacings. At close spacings (1 and 2 ft), a small chisel and hammer were used. A claw hammer was used for a spacing of 4 ft, and a 15-lb sledge hammer was used for spacings equal to or greater than 8 ft.

At each site the last receiver spacing was greater than the length of the slab, and the geophones were located across joints. These joints had a minor effect on the measurements because of the low frequencies (long wavelengths) measured with this spacing. As such, the wavelengths were significantly longer than the depth of the joints, causing negligible disturbance in the wavepath.

Construction of Dispersion Curves

A spectral analyzer was used to record and analyze outputs from the two receivers. After each travel time record from the receivers was captured in the time domain, the signals were transformed into the frequency domain and spectral analyses were performed. The portions of the spectral analyses of interest in SASW testing are the phase information of cross-power spectrum and the coherence function. The coherence function is an indicator of the amount of random background noise at each frequency that is interfering with the actual impact. The coherence is a real-valued function analogous to a signal-to-noise ratio and ranges between zero and one. A coherence of unity at a given frequency can generally be translated into complete elimination of undesirable background noise and total correlation between the signals detected by the two receivers if it is based on the average of several impacts. The phase information of the cross-power spectrum is indica-

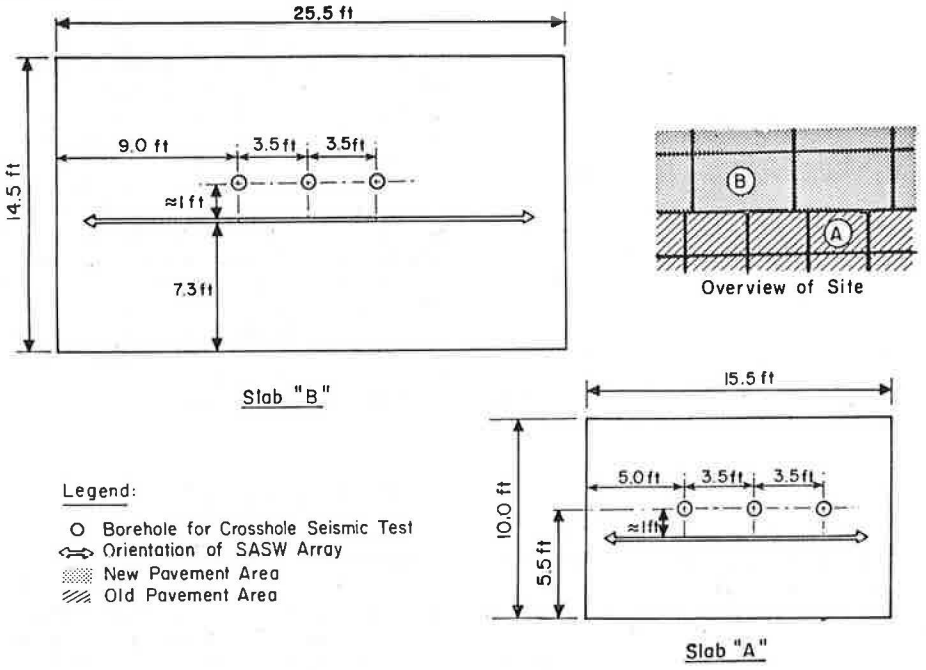

FIGURE 5 Plan view of testing locations.

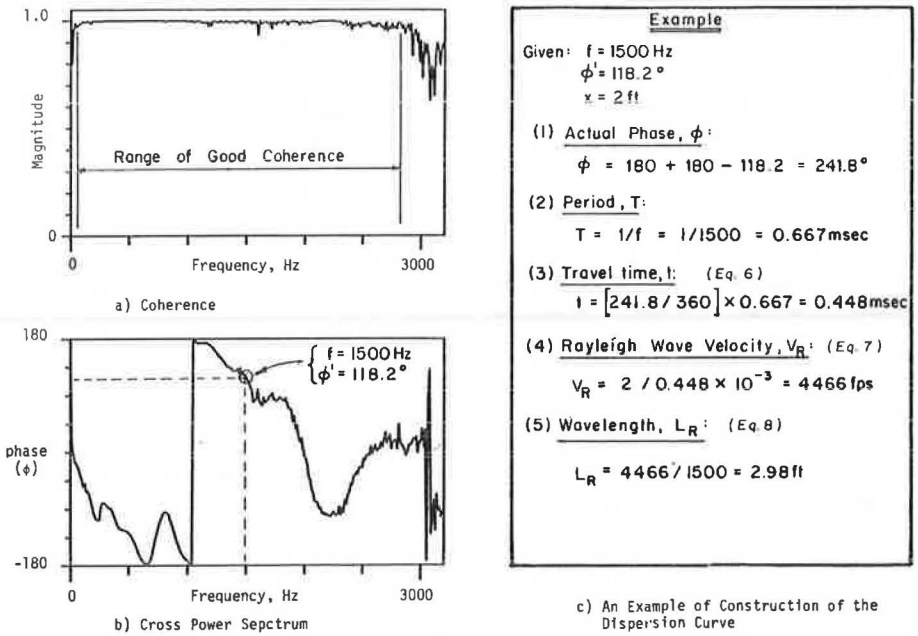

FIGURE 6 Typical coherence and cross-power spectrum used in construction of dispersion curve.

tive of the relative phase difference between signals at each frequency in the range of the measured frequencies.

A typical coherence function and phase information from the cross-power spectrum are shown in Figure 6. From the coherence function, the range of frequencies that should be initially considered in data reduction is chosen. For each frequency in this range the phase shift associated with that frequency is determined by using the phase of cross-power spectrum (Figure 6b). A phase shift equal to 360 degrees corresponds to a travel time equal to one period. As such, the travel time of the Rayleigh wave within the distance between the two receivers for a given frequency (f) can be calculated from

$$t = (\phi/360) \cdot T \quad (6)$$

where

t = travel time of the Rayleigh wave,
ϕ = phase shift, and
T = 1/f = period corresponding to the given frequency (f).

As the distance (X) between the geophones is known, the Rayleigh wave velocity (V_R) for the known frequency (f) is equal to

$$V_R = X/t \quad (7)$$

The wavelength (L_R) associated with frequency (f) is

$$L_R = V_R/f \quad (8)$$

By repeating this procedure for other frequencies on each record, a number of data points (representing R-wave velocity versus wavelength) are obtained, from which the dispersion curve is constructed. A numerical example that uses Equations 6-8 to find the R-wave velocity at one wavelength (frequency) is shown in Figure 6c.

On the basis of studies at several soil sites, Heisey et al. (3) suggested that the distance between receivers (X) should be less than two wavelengths and more than one-third of a wavelength. Based on these criteria, any point with a wavelength less than half of the geophone spacing or more than three times the distance between the geophones is eliminated from construction of the dispersion curve. Fortunately, portions of the dispersion curve from different receiver spacings partially overlap, and the final dispersion curve is continuous.

Dispersion curves from the old and new pavement sections are shown in Figures 7a and 7b, respectively. Scatter in the first few feet of wavelengths is basically because of scaling of the figure. In other words, the scale of the wavelength axis is so large that the data points appear to form horizontal lines. To demonstrate the actual distribution of points, two portions of the dispersion curve for the old pavement (Figure 7a) are shown in Figure 8. Different branches of the dispersion curve can be easily distinguished. These branches represent different modes of Rayleigh waves (9). These modes could not be detected clearly in the earlier work (3) because only a few data points from each cross-power spectrum were picked manually. In the past year construction of dispersion curves has been fully automated. As such, all data points on the digitized records of the cross-power spectrums (which are within the filter criteria) are used. This results in a comprehensive dispersion curve that consists of thousands of data points, as opposed to a few hundred points in the past.

Inversion of Dispersion Curve

Inversion of the dispersion curve (or simply inversion) is the process of determining the layer thicknesses and shear wave velocity profile from the dispersion curve. The most crude type of inversion that has been used for many years is to assume that the sampling depth is equal to one-half to one-third of the wavelength and the shear wave velocity is equal

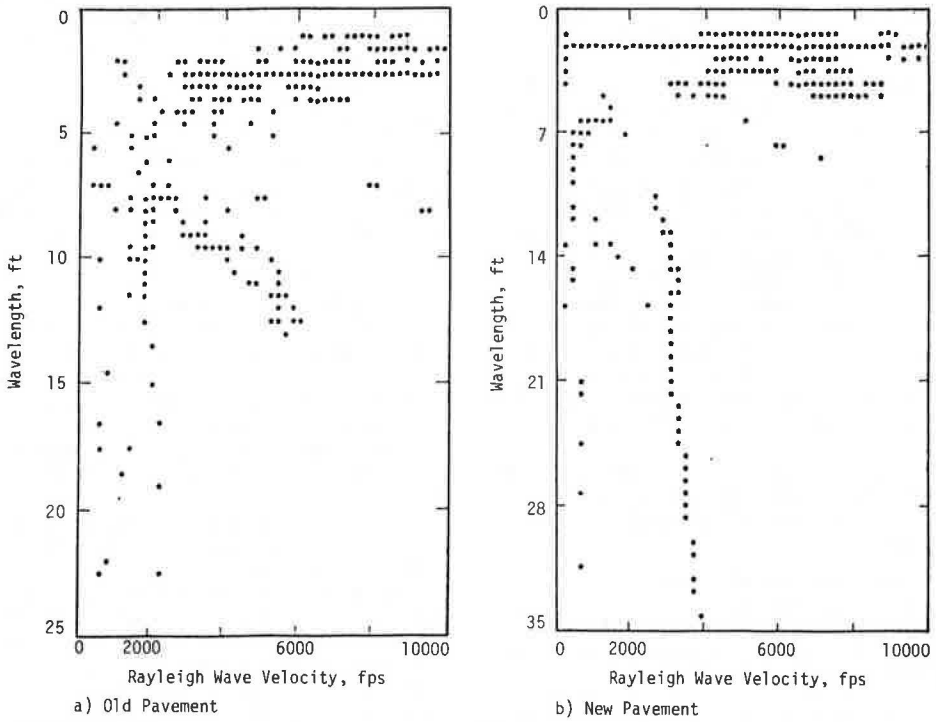

FIGURE 7 Dispersion curves from pavement sections.

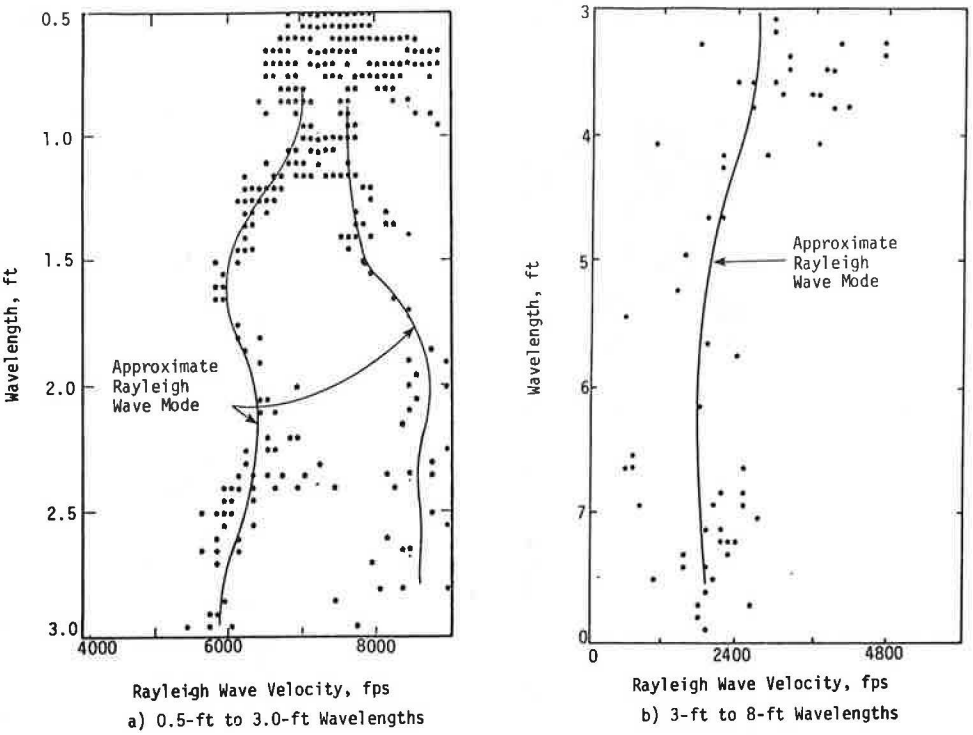

FIGURE 8 Portions of dispersion curve from old pavement section.

to 1.1 times the Rayleigh wave velocity (3,8). In other words, simply multiply the scale of the wavelength axis by one-half or one-third and the scale of Rayleigh wave velocity axis by approximately 1.1 to obtain the S-wave velocity profile. Existence of a layer that has a significantly higher or lower velocity at the surface of the medium affects measurement of the velocities of the underlying layers. As such, R-wave velocities determined by this method are not actual velocities of the layers but are apparent R-wave velocities. Naturally, the shear wave velocity profile determined by this method is in error. However, in a layered medium in which no significant contrast in velocities exists, the apparent and actual R-wave velocities are approximately equal.

Nazarian et al. (4) presented an approximate inversion process. In this process the depths of the layers were assumed to be equal to one-third of the wavelength. Based on Haskell's (10) matrix for elastic surface waves in a layered media and assuming that the apparent and actual R-wave velocities of the top layer are equal, the S-wave velocity profile was constructed from the top to the bottom sequentially.

The new inversion process is rigorous, and all simplifying assumptions made in other techniques (such as sampling depth) are eliminated. The only assumptions are that

1. The layers are horizontal, and thus if any dipping layers exist in the profile the average property of those layers are determined, and
2. The layers are laterally homogeneous over the geophone spacing and are linearly elastic.

The inversion process is based on a modified version of Haskell's (10) and Thompson's (11) matrix for elastic surface waves in a multilayered solid media. In this process shear wave velocities of different layers are assumed and a theoretical dispersion curve, based on this profile, is generated. Poisson's ratios and mass densities are assumed. However, Grant and West (9) and Ewing et al. (12) indicate that the effect of these two parameters on the process of inversion is not significant (especially in the case of pavement materials and soil layers in which these two parameters have reasonably narrow ranges). This theoretical curve is then compared with the experimental dispersion curve constructed from field data. If the two curves agree reasonably well, the shear wave velocity profile is obtained. If the two curves do not match, velocities of the layers are changed, and a new theoretical curve is generated and compared. This iterative process is continued until the two curves (theoretical and experimental dispersion curves) match. It should be mentioned that, as an initial trial, use of the first crude inversion process is advised (especially for soil sites).

To illustrate the matching process, the dispersion curves from the first 8 ft of the old pavement section (Figure 8) are compared in Figure 9 with the theoretical dispersion curves generated with the inversion algorithm. Symbols U and L represent the upper and lower boundaries, respectively, of possible locations of a theoretical data point in the figures. Upper and lower boundaries are displayed (as opposed to a mean value) so that the resolution of the theoretical solution can be interpreted. The symbol O is used to show a perfect match, and the symbol X is used to represent a point where the upper and lower boundaries overlap. As can be seen in Figure 9, the trends in the experimental data follow the theoretical dispersion curves quite closely. At this site the scatter in experimental data was unusually high for unknown reasons. However, the trends are still predicted closely. It is estimated that the accuracy with which R-wave velocities were measured and the use of the inversion process together cause less than a ±10 percent error in shear wave velocities reported herein.

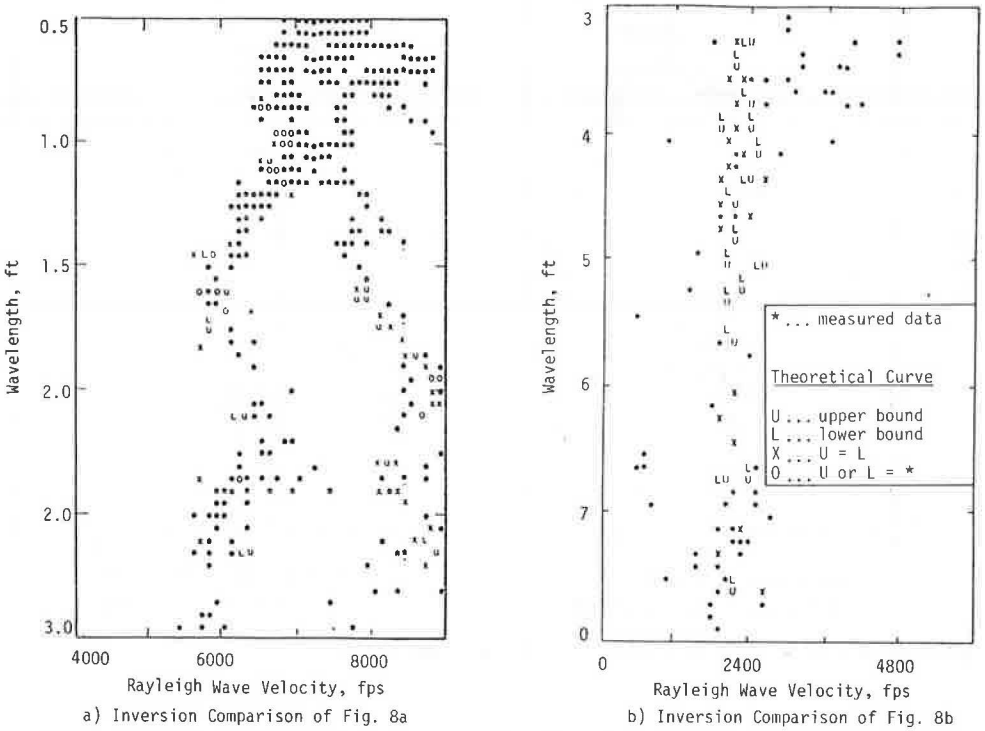

FIGURE 9 Comparison of theoretical and measured portions of dispersion curves from old pavement section.

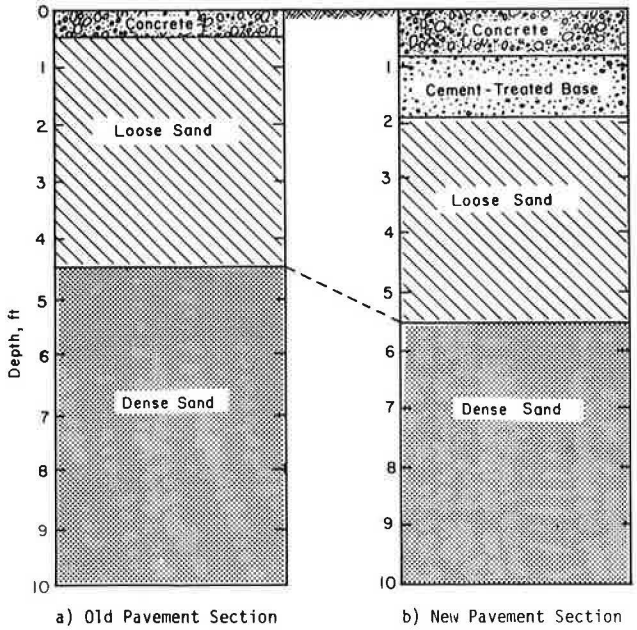

FIGURE 10 Material profile at each test section.

Presentation of Results

As mentioned, two types of seismic tests were performed at the runway sites. With the SASW test, shear wave velocity profiles were first determined. Shear wave velocity and compression wave velocity profiles were obtained with the crosshole test. By knowing shear and compression wave velocities from the crosshole test, values of Poisson's ratio were calculated by using Equation 5.

Soil profiles under the old and new pavements are shown in Figures 10a and 10b, respectively. From the borings for the crosshole tests, the old section was determined to consist of 6 in. of concrete underlain by approximately 4.5 ft of loose gray sand and then dense sand. The material profile at the new pavement section was made up of 10 in. of concrete underlain by approximately 14 in. of cement-stabilized base, which was followed by loose sand underlain by dense sand.

The shear wave velocity profiles of the two sections are shown in Figures 11 and 12. A total of 16 layers was selected in the first 9 ft of the profile to analyze (in the inversion process) the old pavement (Figure 11a). The layer thicknesses became progressively thicker with depth, as the properties of the near-surface materials were most important in this study. The number of layers selected to analyze the new pavement was 18 layers, as shown in Figure 12a. No other NDT method has the ability to enable the user to choose such a fine layering or to have such accuracy.

Also shown in Figures 11 and 12 are the shear wave velocities determined by the crosshole method. In stiff material such as concrete, the crosshole test can have the drawback of not generating measurable shear waves, as was the case in this study. However, the compression wave velocity was obtained very accurately. As such, shear wave velocities determined by the crosshole test in the concrete and the near-surface base material were back-calculated from P-wave velocities assuming Poisson's ratios of 0.15 and 0.25, respectively.

The shear wave velocity profiles shown in Figures 11 and 12 are in excellent agreement. Shear wave velocities from the two methods for the old and new pavement sections are given in Tables 1 and 2, respectively. The average difference between velocities determined by the crosshole and SASW methods is 10 percent at the old pavement and 12 percent at the new pavement.

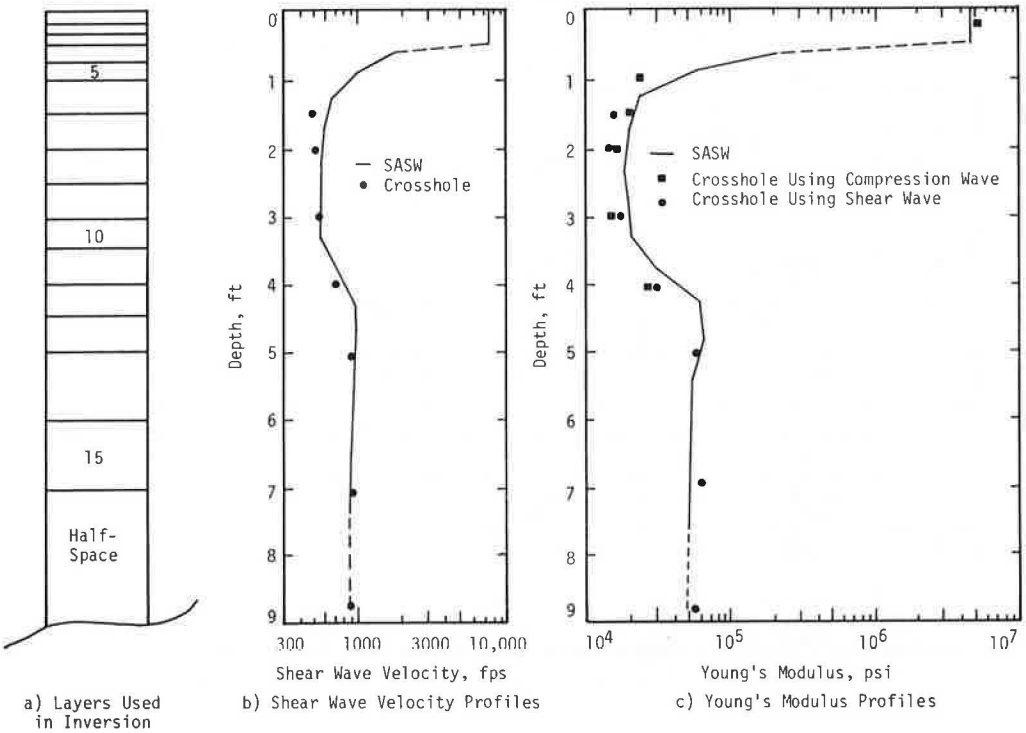

FIGURE 11 Comparison of shear wave velocities and Young's moduli from crosshole and SASW methods at old pavement section.

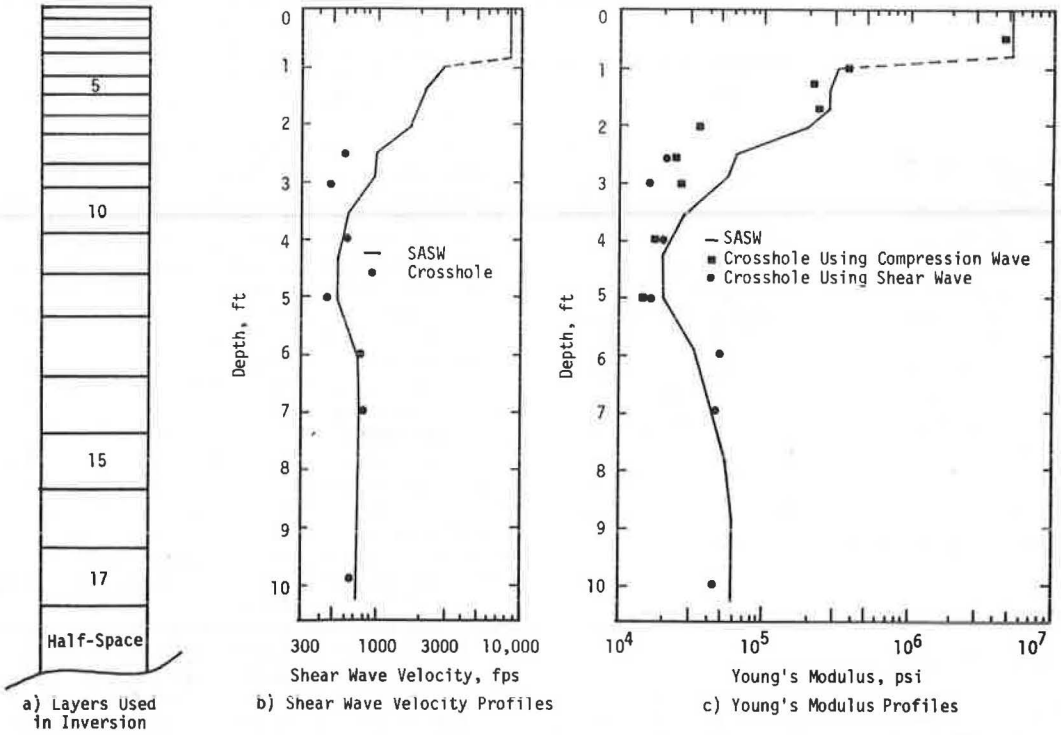

FIGURE 12 Comparison of shear wave velocities and Young's moduli from crosshole and SASW methods at new pavement section.

TABLE 1 Comparison of Wave Velocities from Crosshole Seismic and SASW Tests on Old Pavement Section

Depth (ft)	Shear Wave Velocity		Range of Compression† Wave Velocity from Crosshole Tests (fpc)	Poisson's Ratio		Assumed Unit Weight (pcf)
	Range from Crosshole† Tests	SASW Tests		from† Crosshole Tests	Assumed$^{\Psi}$	
(1)	(2)	(3)	(4)	(5)	(6)	(7)
0.3	-*	7950	11460-13740 [12800]	-*	.15	145
1.0	-*	640	1100-1330 [1210]	-*	.33	110
1.5	436-523 [484]	580	1000-1325 [1145]	.38 - .41 [.39]	.33	110
2.0	476-538 [507]	580	1000-1025 [1012]	.30 - .36 [.33]	.33	110
3.0	538-561 [548]	570	875-1022 [949]	.20 - .28 [.24]	.33	110
4.0	695	700	1311	.30	.33	110
5.0	928	990	5571#	.47	.49	110
7.0	896-1009 [952]	890	5581-5708# [5620]	.49	.49	110
9.0	870-954 [912]	890	5282-5531# [5406]	.49	.49	110

* Inconclusive data
† Numbers in brackets are the average values
# As the soil is saturated, reported compression wave velocities basically represent wave velocities in water, not the soil skeleton
Ψ SASW analysis performed before crosshole data analyzed, therefore Column 5 differs from Column 6

TABLE 2 Comparison of Wave Velocities from Crosshole Seismic and SASW Tests on New Pavement Section

Depth (ft)	Shear Wave Velocity		Range of Compression† Wave Velocity from Crosshole Tests (fpc)	Poisson's Ratio		Assumed Unit Weight (pcf)
	Range from Crosshole† Tests	SASW Tests		from† Crosshole Tests	Assumed$^{\Psi}$	
(1)	(2)	(3)	(4)	(5)	(6)	(7)
0.5	-*	8750	12160-13770 [12736]	-*	.15	145
1.0	-*	2290	3720	-*	.15	145
1.3	-*	2110	3248	-*	.25	125
1.5	-*	2080	3225	-*	.25	125
2.0	-*	1010	1046-1545 [1221]	-*	.25	125
2.5	595	1010	1182	.33	.33	110
3.0	496	950	1271	.24	.33	110
4.0	608-609 [608]	560	954-1121 [1038]	.12 - .29 [.20]	.33	110
5.0	470-511 [496]	560	870-958	.27 - .30	.33	110
6.0	833-933	780	833-933# [883]	.49	.49	110
7.0	783-854 [818]	780	4897-5029# [4963]	.49	.49	110
10.0	783-816 [799]	837	5262-5123#	.49	.49	110

* Inconclusive data
† Numbers in brackets are the average values
# As the soil is saturated, reported compression wave velocities basically represent wave velocities in water, not the soil skeleton
Ψ SASW analysis performed before crosshole data analyzed, therefore Column 5 different from Column 6

Determination of Elastic Moduli

Once the propagation velocities of each layer have been determined, Young's moduli and shear moduli can be easily calculated. In the case of the SASW method, the shear wave velocities are determined from which shear moduli (G) are calculated by using Equation 2. Young's modulus and shear modulus are related through Poisson's ratio by

$$E = 2(1 + \nu)G \qquad (9)$$

In crosshole tests both shear and compression wave velocities are determined. Therefore, Young's modulus can be calculated from either Equation 3 or 5.

Young's modulus profiles from the old and new pavements are shown in Figures 11 and 12, respectively. The profiles obtained from the crosshole and SASW tests are in good agreement, except in the range of 2 to 3 ft, over which some scatter exists. The assumed mass densities and Poisson's ratios and calculated Young's moduli are presented in Tables 3 and 4. The excellent agreement between the profiles from these two independent testing techniques illustrates the value and versatility of the SASW method.

SUMMARY AND CONCLUSIONS

Nondestructive testing of rigid pavement with the SASW method is discussed. This method has been under continuous development during the past few years. Construction of dispersion curves from data collected in situ is fully automated, resulting in a comprehensive dispersion curve consisting of thousands of data points. As a result, different modes of the Rayleigh wave can now be detected, serving as a multiple check on the accuracy of the data reduction.

A new, rigorous inversion process has been developed that eliminates all significant simplifying assumptions used in the past. This new inversion process was applied to data collected at two airport runway sites. Young's modulus profiles obtained by the SASW method illustrate the power of this method in determining fine layering in the pavement section with excellent accuracy. Also, Young's modulus profiles agreed closely with those determined by the well-established crosshole seismic method.

In the aspect of automation, the SASW technique is still in research and development stages. Once the system is automated, it would be just as fast to perform a test in situ with this method as any other NDT method carried out today. In addition, the method has the advantage of developing a unique profile and determining layer thicknesses with great accuracy.

ACKNOWLEDGMENTS

This work was supported by the Texas State Department of Highways and Public Transportation (TSDHPT) under research 3-8-79-256 and by the U.S. Air Force. The authors wish to thank the personnel of these two organizations, especially Lt. Colonel B. Tolson and Captain J.D. Wilson of Tyndall AFB and G. Peck and R.B. Rogers of TSDHPT. The technical assistance and funding provided by the U.S. Air Force and TSDHPT are sincerely appreciated. Thanks are also extended to Tony Ni, research assistant at the University of Texas, for performing the resonant column tests.

TABLE 3 Comparison of Young's Moduli from Crosshole Seismic and SASW Tests on Old Pavement Section

Depth (ft)	Young's Modulus (psi)			Difference (percent)	
	SASW	Crosshole		$\frac{(2)-(3)}{(2)}$ † (range)	$\frac{(2)-(4)}{(2)}$ † (range)
		Using Compression† Wave Velocity (range)	Using Shear† Wave Velocity (range)		
(1)	(2)	(3)	(4)	(5)	(6)
0.3	4.55×10^6	$(4.11\text{-}5.90) \times 10^6$ [5.14×10^6]	-*	9.7 - 29.7 [13.1]	-*
1.0	2.6×10^4	$(1.95\text{-}2.84) \times 10^4$ [2.35×10^4]	-*	7.0 - 25.0 [9.6]	-*
1.5	2.13×10^4	$(1.60\text{-}2.81) \times 10^4$ [2.13×10^4]	$(1.26\text{-}1.83) \times 10^4$ [1.56×10^4]	9.0 - 24.9 [0.0]	14.1 - 40.8 [26.9]
2.0	2.13×10^4	$(1.60\text{-}1.68) \times 10^4$ [1.64×10^4]	$(1.46\text{-}1.79) \times 10^4$ [1.63×10^4]	21.1 - 24.9 [23.0]	16.0 - 31.5 [23.5]
3.0	2.06×10^4	$(1.23\text{-}1.67) \times 10^4$ [1.45×10^4]	$(1.63\text{-}1.91) \times 10^4$ [1.77×10^4]	18.9 - 40.3 [29.6]	7.3 - 20.9 [14.1]
4.0	3.13×10^4	2.75×10^4	2.98×10^4	12.1	4.8
5.0	6.91×10^4	-#	6.01×10^4	- #	13.0
7.0	5.62×10^4	-#	$(5.68\text{-}7.09) \times 10^4$ [6.39×10^4]	- #	1.1 - 26.2 [13.7]
9.0	5.62×10^4	-#	$(5.35\text{-}6.39) \times 10^4$ [5.87×10^4]	- #	4.8 - 13.7 [4.4]

* Inconclusive data
† Numbers in brackets are the average values
# As the soil is saturated, reported compression wave velocities basically represent wave velocities in water, not the soil skeleton

TABLE 4 Comparison of Young's Moduli from Crosshole Seismic and SASW Tests on New Pavement Section

Depth (ft)	Young's Modulus (psi)			Difference (percent)	
	SASW	Crosshole		$\frac{(2)-(3)}{(2)}$ † (range)	$\frac{(2)-(4)}{(2)}$ † (range)
		Using Compression† Wave Velocity (range)	Using Shear† Wave Velocity (range)		
(1)	(2)	(3)	(4)	(5)	
0.5	5.51×10^6	$(4.62\text{-}5.93) \times 10^6$ [5.09×10^6]	-*	7.6 - 16.2 [7.7]	-*
1.0	3.55×10^5	3.73×10^5	-*	5.1	-*
1.3	3.00×10^5	2.37×10^5	-*	21.4	-*
1.5	2.93×10^5	2.8×10^5	-*	4.4	-*
2.0	6.42×10^4	$(2.46\text{-}5.36) \times 10^4$ [3.47×10^4]	-*	61.7 - 16.5 [45.9]	-*
2.5	6.42×10^4	2.24×10^4	2.23×10^4	65.1	65.3
3.0	2.83×10^4	2.59×10^4	1.58×10^4	8.5	44.2
4.0	1.99×10^4	$(1.46\text{-}2.01) \times 10^4$ [1.74×10^4]	$(1.96\text{-}2.27) \times 10^4$ [2.12×10^4]	26.1 - 1.0 [17.8]	1.51 - 14.1 [6.3]
5.0	1.99×10^4	$(1.21\text{-}1.47) \times 10^4$ [1.34×10^4]	$(1.39\text{-}1.61) \times 10^4$ [1.50×10^4]	26.1 - 39.2 [32.7]	19.1 - 30.2 [24.6]
6.0	4.30×10^4	-#	$(4.91\text{-}6.15) \times 10^4$ [5.53×10^4]	-#	13.4 - 42.0 [27.7]
7.0	4.30×10^4	-#	$(4.33\text{-}5.12) \times 10^4$ [4.73×10^4]	-#	0.7 - 19.1 [9.9]
10.0	5.11×10	-#	$(4.33\text{-}4.70) \times 10^4$ [4.52×10^4]	-#	15.3 - 7.8 [11.6]

* Inconclusive data
† Numbers in brackets are the average values
# As the soil is satruated, reported compression wave velocities basically represent wave velocities in water, not the soil skeleton

REFERENCES

1. J.P. Nielsen and G.T. Baird. Air Force System for Nondestructive Testing of Pavements. Presented at Symposium on Nondestructive Test and Evaluation of Airport Pavements, Vicksburg, Miss., Nov. 18-20, 1975.
2. J.P. Nielsen and G.T. Baird. Evaluation of an Impulse Testing Technique for Nondestructive Testing of Pavements and Recommended Follow-On Research. Report CEEDO-TR-77-46. U.S. Air Force Civil and Environmental Engineering Office, Tyndall Air Force Base, Fla., Sept. 1977.
3. J.S. Heisey, K.H. Stokoe II, and A.H. Meyer. Moduli of Pavement Systems from Spectral Analysis of Surface Waves. In Transportation Research Record 852, TRB, National Research Council, Washington, D.C., 1982, pp. 22-31.
4. S. Nazarian, K.H. Stokoe II, and W.R. Hudson. Use of Spectral Analysis of Surface Waves Method for Determination of Moduli and Thicknesses of Pavement Systems. In Transportation Research Record 930, TRB, National Research Council, Washington, D.C., 1983, pp. 38-45.
5. S. Nazarian and K.H. Stokoe II. Evaluation of Moduli and Thicknesses of Pavement Systems by SASW Method. Report 256-4. Texas State Department of Highways and Public Transportation, Austin, 1982.
6. K.H. Stokoe II and S. Nazarian. Effectiveness of Ground Improvement from Spectral Analysis of Surface Waves. Proc., 8th European Conference on Soil Mechanics and Foundation Engineering, Helsinki, Finland, May 1983.
7. K.H. Stokoe II and R.J. Hoar. Variables Affecting In Situ Seismic Measurements. Proc., ASCE Conference on Earthquake Engineering and Soil Mechanics, Pasadena, Calif., 1978, Volume II, pp. 919-939.
8. F.E. Richart, Jr., J.R. Hall, Jr., and R.D. Woods. Vibration of Soils and Foundations. Prentice-Hall, Englewood Cliffs, N.J., 1970.
9. F.S. Grant and G.F. West. Interpretation Theory in Applied Geophysics. McGraw-Hill, New York, 1965.
10. N.A. Haskell. The Dispersion of Surface Waves in Multilayered Media. Bull., Seismological Society of America, Vol. 43, No. 1, 1953, pp. 17-34.
11. W.T. Thompson. Transmission of Elastic Waves Through a Stratified Solid Medium. Journal of Applied Physics, Vol. 21, Feb. 1950, pp. 89-93.
12. W.M. Ewing, W.S. Jordetsky, and F. Press. Elastic Waves in Layered Media. McGraw-Hill, New York, 1957.

Publication of this paper sponsored by Committee on Pavement Rehabilitation.